Periodicals of Engineering and Natural Sciences ISSN 2303-4521
Vol. 8, No. 4, December 2020, pp.2389-2404

Punching strength behavior of reinforced concrete slabs with chips waste tire rubber

Firas Nadhim Sahib[1], Hayder M.K. Al-Mutairee[2]
[1]M.Sc. Student, College of Engineering, University of Babylon, Hilla, Babil, Iraq.
[2]Professor, College of Engineering, University of Babylon, Hilla, Babil, Iraq.

ABSTRACT

Every year waste in millions of tons is accumulated in the globe and much of it is non-biodegradable in nature, e.g., waste vehicle tires. In addition, waste recycling is energy consuming and pollution producing. Moreover, in this research, an experimental study is carried out to explore the behavior of chips rubberized concrete (CRC) in punching shear of flat plates. The experimental program comprises 10 specimens designed to fail by punching. The investigated parameters were the model type column, chips rubber ratio that used instead of coarse aggregate. Two cases are classified according to shape of column; square and rectangular. Each case consists of five specimens, the first specimen casted by normal strength concrete (NSC) and the other casted with CRC, by 5%, 10%, 15%, and 20%. The experimental results present that increasing chips rubber instead of coarse aggregate in two cases studies (square, and rectangular column) from zero to 20% shows a drop in the punching shear capacity by range of 13.54%, and 18.52%, and a reduction in the initial and secant stiffness by (16.06%, 25.19%), and (24.44%, 26.88%) respectively. Also, using 20% chips waste rubber increased the central deflection of two cases at service load by (37.39%, 47.28%), and increased the central ultimate deflection of the plates by about (24%, 24.58%) respectively. Furthermore, 20% replacement of coarse aggregate by rubber increased the ductility by (20.38%, 15.60%), and increased the energy absorption index significantly by 41.41%, and 28.75%, and led to decrease cracks width at service load by 36.11%, and 44.12% for the two cases respectively. From comparison between theoretical and experimental results one can get three equations relate the deficiency of punching shear capacity and chips rubber ratio, and concluded that the optimal replacement was by using 10% to15%. It can be inferred that the experimental results for square columns (S-R) specimens at all replacement percentages from zero to 20% less constrictive than ACI-code equations, whereas for rectangular columns (R-R) specimens the ACI-code equations can be used to replace 15%, after that the correction factor must be applied

Keywords: Flat Plate, Punching Strength, Rubberized Concrete, Different Column shape, Coarse aggregate replacement.

Corresponding Author:

Firas Nadhim Sahib
College of Engineering, University of Babylon
Hilla, Babil, Iraq
firaseng84@gmail.com

1. Introduction

In multi-story facilities like apartment buildings and parking spaces, flat plates are commonly utilized. A flat slab foundation is constructed only of interconnected slabs and columns. Concrete flat slab floors offer an elegant design type that simplifies and accelerates site processes, enables room to be conveniently and flexibly separated and lowers the average height of buildings [1], [2]. A spatial occurrence that typically happens in a fragile manner, at localized load or column support locations, is punching shear failure. This form of failure is disastrous when no external, observable symptoms are seen before the failure happens, so it was of great concern to engineers to attempt to explain the actions of connections to the slab column. Nevertheless, while the punching shear power of slabs has been thoroughly studied, there is still no widely applicable logical theory to date. Empirical tests are focused on the latest building code construction protocols and questions were posed regarding their capacity to correctly estimate the punching shear power of slabs for al1 circumstances [3]. Punching shear of flat plate which has one column were interested by several researches [4]–[6].

Aggregates (coarse and fine one) are one of the essential materials utilized in concrete manufacturing, but these materials are likely to become scarce. The utilize of rubber in concrete can be seen as a positive step toward sustainable concrete production [4], [6]. It is probable to obtain rubberizing concrete by applying rubber scrap tires to the concrete mixtures. Coarse and fine aggregate has been substituted with rubber from tires waste. The waste of tires rubber are the primary waste materials utilized to produce concrete rubbery [9]–[12]. CRC and

Crumbed rubberizing concrete made by replacing coarse and fine aggregate, respectively, with particles of rubber if mixing concrete, the substantial aims to reduce convinced environmentally influences substantially, but their structural characteristics are stayed moderately unfamiliar [13], [14].

Many researchers [15]–[17] found that the characteristics of split tensile strength sand flexural are significantly reduced at a slow average compared to compressive strength. As foretell, the strength of cement composites thereafter enhanced with the reduction of tire rubber and the act that strength mechanically is strictly connected with the dynamic module of elasticity. While the others [17]–[19] found out that the bonding between the rubber elements and the matrix can be achieved by several ways. As much as styrene butadiene rubber is disrupted by liquid and anionic bitumen suspension, microscopic studies have demonstrated that these kinds of extracts are well bound to the surface of rubber particles, thereby reinforcing the bond between cement mortar, aggregate additives, and rubber particles. Sambucci, et al., [20] observed that the ductility in the stress against strain relationship improved with the inclusion of particles from wastes-rubber and the rise of particles. The index of brittleness BI was calculated to predict concrete ductility. If the amount of waste tire rubber was 10 per cent, the top magnitude has been provided. Following this percentage, the failure modes change from fragile to ductile. The decrease in the BI above 10% contributes to a rise in plastic energy.

However, the current study focused on the punching strength and behavior of CRC flatted plate using different tire rubber waste as a coarse aggregate replacement, experimentally with absence of shear reinforcement. As well as it investigate the effect of the column shape on the punching shear behavior of the plate that produced with CRC in different tire waste ratios.

1. Experimental part

1.1. Materials

Ordinary Portland cement (Made in Iraq by Lafarge Company) called (KARASTA) has been utilized for casting all the samples in this investigation. Table 1 and 2, demonstrate the chemical composition and physical characteristics of cement, which was compatible with Iraqi Code Requirement (IQS No.5/1984) [21]. In this investigation, natural sand of a maximum size of 4.75 mm has been utilized from Al-AKhaider sand source as a fine aggregate. While the semi-crushed gravel of 10 mm as a maximum size has been utilized as a coarse aggregate. Pre-using both types of aggregate, they washed and cleaned by water several times, later it was spread out and left to dry in the air to prevent the accumulation of humidity which can significantly affect water content for mix of concrete. Waste chips tire rubber with size (4-10) mm was supplied by General Company for Rubber Industries and Tires/ governorate of Al-Najaf al-Ashraf in Al-Hadiaria city, it was utilized as a coarse aggregate replacement material. Physical and chemical characteristics of aggregates in depending with the Iraqi Requirement (IQS No.45/1984) [22] and ASTM C33-03 [23], as tabulated in Tables 3, 4 and 5. For completing the concrete mixture. Spigot water was utilized in curing as well as casting of all the specimens. For reinforcing the concrete slabs and columns, one size of deformed steel reinforcement Ø10mm has been used, the bars of steel reinforcement for this diameter were tested at the Material Engineering Laboratory at Babylon University. Table 6 shows the results of Steel bars properties that obtained from testing. Steel reinforcement tensile test was conducted for three samples according to ASTM A615 [24].

Table 1. Chemical composition and main compounds of the cement utilized

Oxide composition	Abbreviation	%-by weight	Limit of IQS NO. 5/1984
Lime	CaO	62.77	-
Silica	SiO2	20.54	-
Alumina	Al2O3	5.60	-
Iron oxide	Fe2O3	3.29	-
Sulphate	SO3	2.34	≤2.5% if C3A< 5% ≤2.8% if C3A> 5%
Magnesia	MgO	2.80	≤5%
Loss on Ignition	L.O.I.	1.95	≤4%
Lime saturation factor	L.S.F.	0.91	0.66-1.02
Insoluble residue	I.R.	1.21	≤ 1.5
Main compounds (Bouge's eq.)		% by weight of cement	
Tricalium silicate (C3S)		50.14	----------
Diacalcium siliccat (C2S)		19.05	----------
Trialcium aluminate (C3A)		3.25	≤ 3.5 %
Tetracalcium aluminoferrite (C4AF)		10.11	----------

Table 2. Physical characteristics of cement utilized

Setting Time, (min) **Initial** **Final**	**123** **195**	**≥ 45** **≤ 600**
Fineness (Blaine), m² /kg	315	≥ 230
Compressive Strength ,(MPa) **3days** **7days**	 27.52 38.4	 ≥ 15 ≥ 23

Table 3. Grading of the utilized aggregates and rubber

Sieve size (mm)	**Fine aggregate**		**Coarse aggregate**		**Waste Tires Rubber***	
	Percentage passed	**Limits of IQS. No. 45/1984**	**Percentage passed**	**Limits of ASTM C 33/2003 (1.18 to 9.5 mm)**	**Percentage passed**	**Limits of ASTM C 33/2003 (1.18 to 9.5 mm)**
12.5	-	-	100	90---100	100	100
9.5	-	-	92	90---100	91	90-100
4.75	96	90---100	12	10---30	24	20-55
2.36	79	75---100	1.8	0---10	13	5-30
1.18	62	55---90	0.8	0---5	0.1	0-10
0.6	41	35---59	-	-	-	-
0.3	15	8---30	-	-	-	-
0.15	3	0---10	-	-	-	-

Table 4. Physical and chemical characteristics of the utilized aggregates and rubber

Characteristics	**Fine aggregate**		**Coarse aggregate**		**Rubber**
	Test consequences	**Limits of IQS. No. 45/1984**	**Test consequences**	**Limits of IQS. No. 45/1984**	
Specific gravity	2.64	--	2.65	--	1.78
Fineness modulus	2.70	--	--	--	3.14
Absorption %	0.74	--	0.77	--	2%
Sulfate content (SO3) %	0.12	(max ≤ 0.5%)	0.08	Requirements up to 0.1% (max.)	
Density	--	---	--	--	511.2 (kg/m3)

Table 5. Chemical composition of the rubber utilized

Major Rubber Components	**Consequences%**
Natural rubber content	31
Carbon black content	30
Ruber hydrocarbon	25
Acetone extract	10
Ash content	4

Table 6. The consequences of test steel bars utilized *

Nominal diameter (mm)	Measured diameter (mm)	Area (mm^2)	Max. Elongation (%)	Yield tensile stress (Mpa) (fy)	Ultimate tensile stress (fu) (*MPa*)	Modulus of elasticity (*MPa*)
10	9.73	74.355	12.44	511	689	200000

***** Each magnitude is an average of three samples (each one has 40 cm length).

1.2. Mix design of normal and rubberized concrete

To ensure the required concrete characteristics the next design was adopted to make NSC. The mix was designed in depending to (ACI-211-02) [25], (mix design with nominal compressive strength of fc'=35MPa at 28 day). Mixture details are given in Table 7. It was found that the utilized mixture produces good workability and uniform mixing of concrete with absence segregation. The quantities of water, cement and fine aggregate are fixed constant as (536.69, 205.66 and 768.5) kg/m^3 respectively.

1.3. Samples details and fabrication

1.3.1. Details

The experimental program comprises 10 flat plates that are built to simulate interior slab-column connections. The slab's dimensions are 900 mm × 900 mm ×80 mm represent models on a scale of 1/3 with respect to a real multi-story structure as multi-bay prototype building structure. The one-third (for column strip) of the scale factor was utilized to cast a square slab with 900-mm side length taking into account the supporting clarity with similarly spaced at distance of 4800 mm (center to center) in both directions, as illustrated in Figure (1). Figure (2**)** and Figure (3) show details of square and rectangular columns samples. The samples were divided into five groups (G1, G2, G3, G4 and G5) depending on the ratio of replacement, and the details of each group was mentioned in Table 7, each group consists of two specimens depending on columns shape (square= S, and rectangular=R).

Table 7. Details of constituents of the trail mixes*

Group No.	Mixes	Column Shape	Sample Description	Coarse Aggregate (kg/m^3)	Chip Rubber (kg/m^3)	Total weight (kg/m^3)
G1	CRC0%	Square	S-R0	808.5	0	2319.35
		Rectangular	R-R0			
G2	CRC5%	Square	S-R5	768.075	12.5	2291.43
		Rectangular	R-R5			
G3	CRC10%	Square	S-R10	727.65	25	2263.50
		Rectangular	R-R10			
G4	CRC15%	Square	S-R15	687.225	37.5	2235.58
		Rectangular	R-R15			
G5	CRC20%	Square	S-R20	646.8	50	2207.65
		Rectangular	R-R20			

* all quantities are in **kg/m^3**.

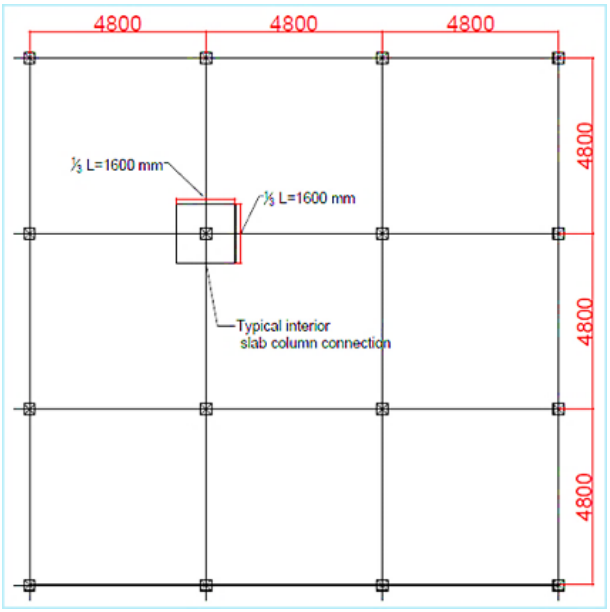

Figure 1. The portion of slab under consideration in a typical flat plate floor plan (all dimension in mm).

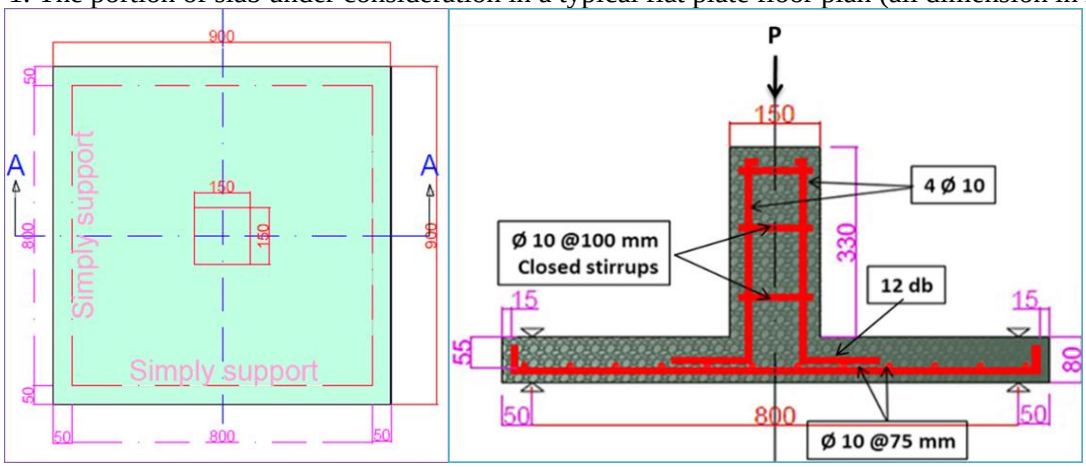

a) Plan samples of S-R model b-Typical reinforcement for S-R samples

Figure 2. Details of square columns samples.

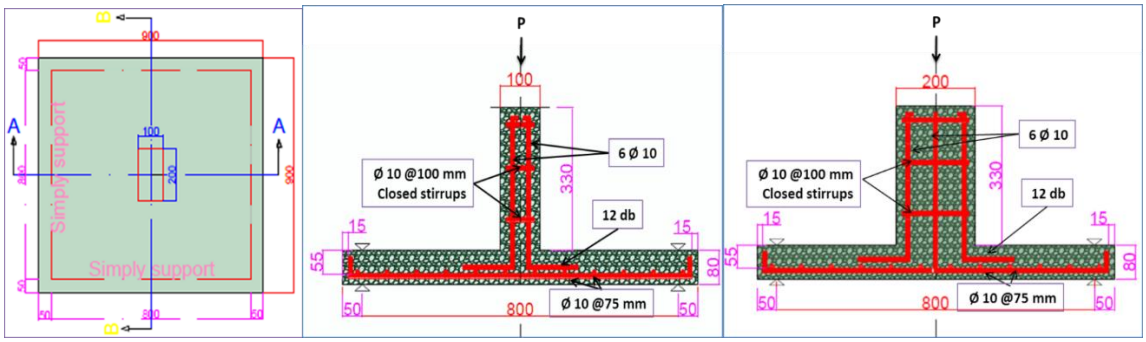

a) Plan samples of R-R model. b) Typical reinforcement section A-A. c) Typical reinforcement section B-B.

Figure 3. Details of rectangular columns samples

1.3.2. Fabrication

A wooden mold that consists of base plywood plates and sides of lumber were fixed together well with screws and can be opened and installed in a way to confirm having a double net inside area of 900 mm × 900 mm were utilized. As well-known process that include oiling the mold and placing the plastic spacers were implemented before placing the concrete in the molds. Also, plywood molds with dimensions (15 x 15 x 33 cm) and (10 x 20 x 33 cm) as shown in Figures (4 and 5) were utilized for the square and rectangular column, respectively. After casting, a humid curing was maintained by covered the sample by nylon sheets for the first 24 hours depending

to the recommendations of ACI 308R-01 [10] while the curing conditions were applied for 28-days after casting in compliance with ASTM C 192/C192M-05 [11] and ACI-363R-97 [12].

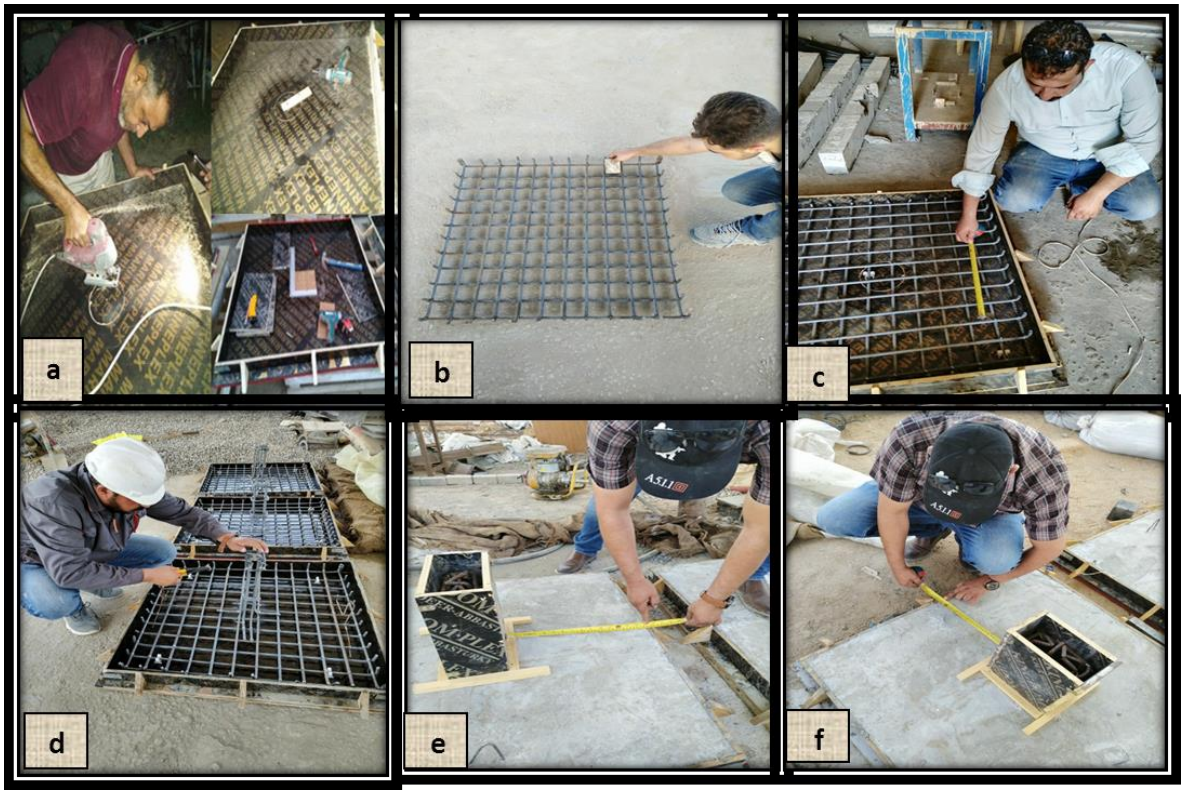

Figure 4. Molds preparing

Figure 5. Samples, casting and curing

1.4. Testing the samples

The testing procedure, as shown in Figure 6, consists of mega electrical pressure transducer was utilized to measure the applied load. While the deflections at different locations on the tension side have been determined using 4 gauges (dial one) with correctness (0.001 cm) and determining capacity (30 mm). The locations of the dial gauges were chosen to measure the maximum deflection at the column center and some other positions. A microscope with 0.002 cm correctness has been utilized to measure the width of cracks at the service load. Surveillance cameras system are utilized to record the consequences in this study. Four cameras were directed to the dial gauges and one camera on the load display to get the load-deflection curve for a slab. The video was

stopped at a particular load to obtain the readings of the dial gauges. Figures 7 and 8 explain the procedure for marking the cracks patterns at failure of specimens.

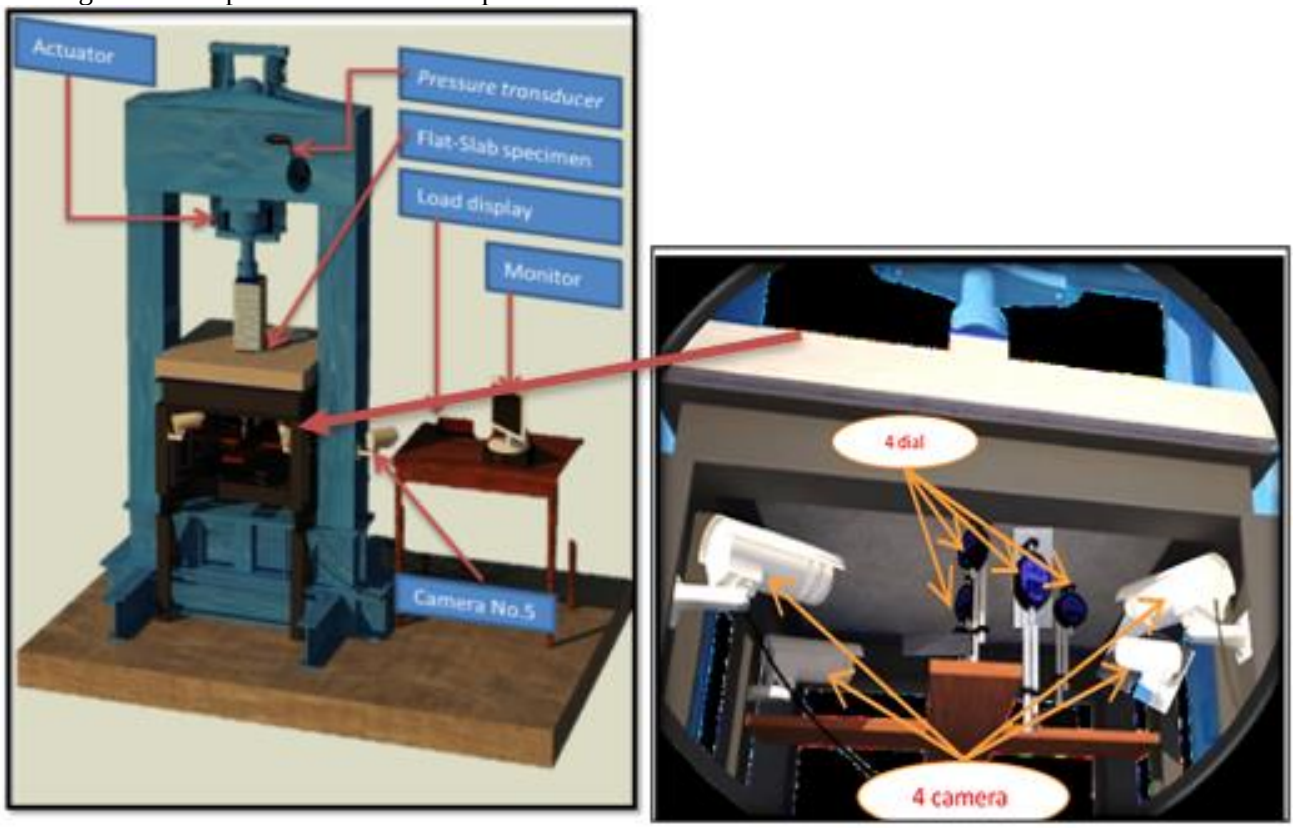

Figure 6. Testing setup

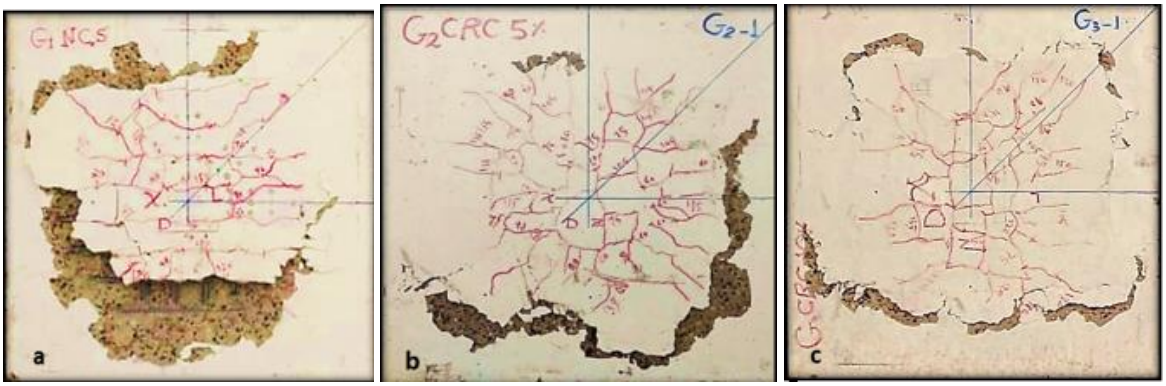

a) S-R0 b) S-R5 c) S-R10

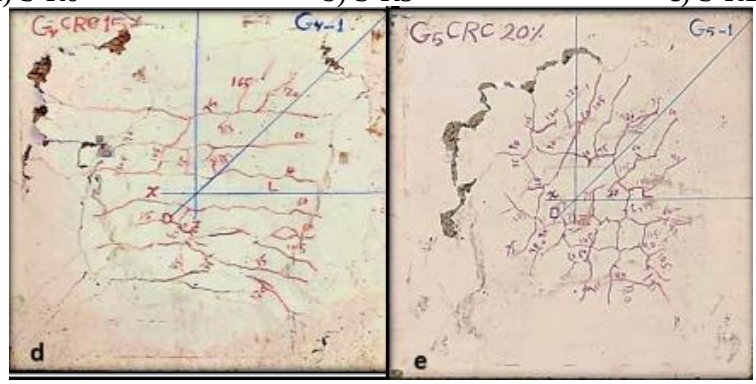

d) S-R15 e) S-R20

Figure 7. Crack patterns at failure of specimens S-R

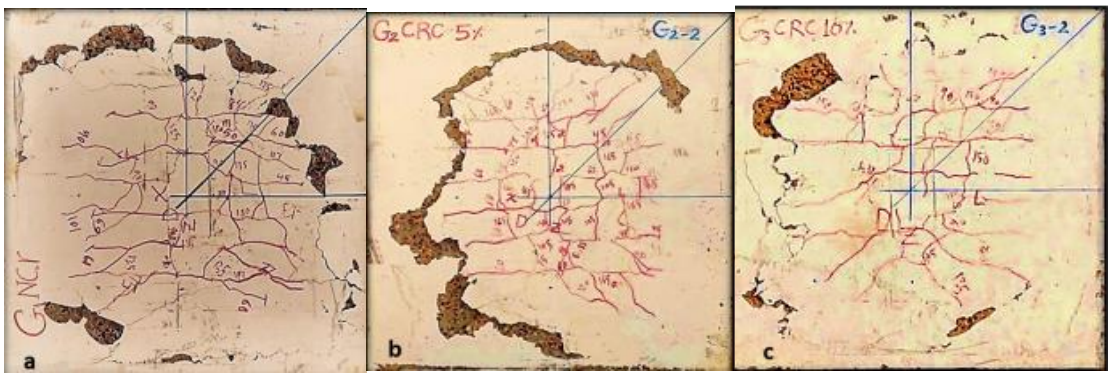

a) R-R0 b) R-R5 c) R-R10

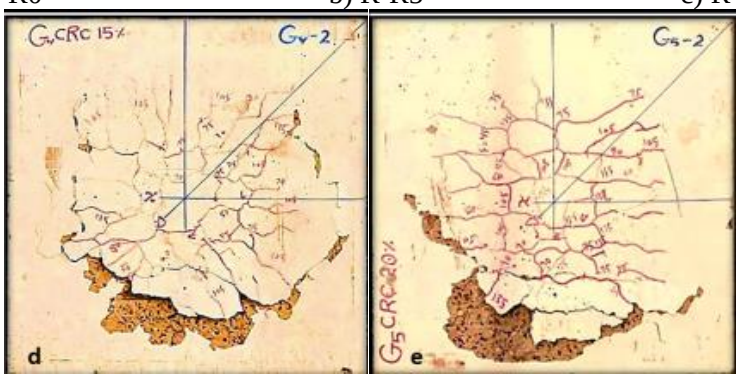

d) R-R15 e) R-R20

Figure 8. Crack patterns at failure of specimens R-R

2. Results and discussions

2.1. Load - deflection

The deflections of each model specimens are computed in four different places on the specimen surface axes of flat plates at (mid-center, x-axis, z-axis and diagonal d- axis) by using four dial gauges. Table 8 contains the cracking and ultimate loads and the matching deflection at first cracking. The compressive strength was decreased after replacing coarse aggregate, which compatible with decreasing first crack load and the decreasing ratio increased with increasing the replacement ratio. However, the first crack deflection results show an increasing with increasing the waste tires ratios for both columns shape, but the square shape give better results comparison with rectangular shape.

Table 8. Experimental results of tested slabs

Group No.	Specimen	Compressive Strength	First Crack Load	First Crack Def.	Ult. L.	Diff. % of Ult. L.	Ult. Central Def.	Diff. % of Ult. Central Deflection	Crack Width at Service Load
		fc'	*fcr*	Δcr	Pu		Δu		ws
		MPa	*kN*	*mm*	*kN*		*mm*		*mm*
G1*	S-R0	35.54	43.8	1.04	198.5	0.00	6.75	0.00	0.36
G2	S-R5	33.09	41.17	1.09	192.05	-3.25	7.23	7.11	0.33
G3	S-R10	28.21	39.54	1.28	184.37	-7.12	7.58	12.30	0.28
G4	S-R15	27.21	37.79	1.07	178.71	-9.97	7.80	15.56	0.26
G5	S-R20	24.87	35.78	1.24	171.62	-13.54	8.37	24.00	0.23
G1*	R-R0	34.92	40.5	0.79	193.84	0.00	6.02	0.00	0.34
G2	R-R5	31.17	38.8	0.91	187.52	-3.31	6.23	3.49	0.3
G3	R-R10	28.55	37	0.87	179.84	-7.27	6.54	8.64	0.25
G4	R-R15	26.83	35.4	0.93	169.67	-12.51	6.88	14.29	0.22
G5	R-R20	25.31	33.2	0.97	157.94	-18.52	7.50	24.58	0.19

Ult.= ultimate, L= load, Def.= deflection.

2.2. Central deflection and ultimate loads of specimens

From Figure 9 (a & b) shows that effect of replacing the coarse aggregate by chips of waste tire rubbers with ratios 5%, 10%, 15%, and 20%, on the load-deflection curves. Figure 9(a) present five specimens S-R0, S-R5, S-R10, S-R15, and S-R20 (square column) tested under central load. It can be observed that increasing the chips rubber of the replaced instead of the coarse aggregate led up to an increase in the central deflection at similar level of load. Increasing the percentage of chips rubber from 0% to 20% was increased the central deflection by 45.64% at a level of load 171.62 kN, and increased the ultimate central deflection by 24% as well as produces a reduction in the punching load capacity by 13.54%. While in Figure 9 (b) presents five specimens R-R0, R-R5, R-R10, R-R15, and R-R20 are tested under central load (rectangle column). It can be observed that increasing the chips rubber of the replaced instead of the coarse aggregate led up to an increase in the central deflection at similar level of load. Increasing the percentage of chips rubber from 0% to 20% produces increment in the central deflection by 56.08% at a level of load 157.94 kN, while increased the ultimate central deflection by 24.58% and yields a reduction in the punching load capacity by 18.52%, respectively.

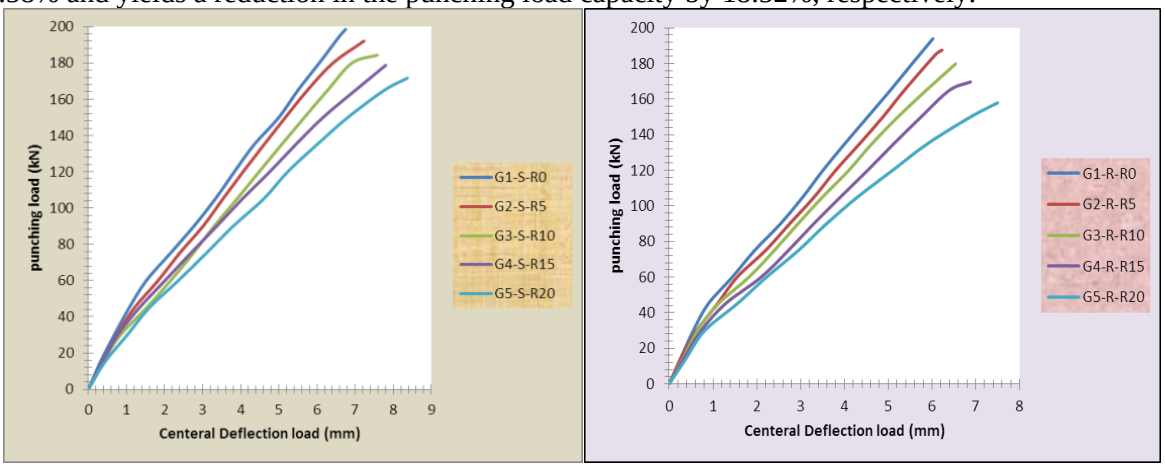

a) S-R specimens b) R-R specimens

Figure 9. The load-central deflection curves

2.3. Stiffness of the tested specimens

As a result, the initial stiffness has been determined as the proportion of the final load (Pu) of the slabs to the yielding displacement (Δ**y**) and, in the same way, the secant stiffness was determined by the proportion of the yielding load (Py) to the yielding disp. (Δ**y**). The yielding load (Py) weighed as the load conformable to the estimated yielding displacement of the load-displacement curve of any specimen. The uncracked stiffness and post-cracking stiffness of all the specimens as shown in Figure (10). The uncracked and cracked stiffness were significantly affected by using the waste of chips tire rubber instead of coarse aggregate. Increase percentage of chips rubber to 5%, 10%, 15%, and 20% instead of coarse aggregate volumetrically in specimens (S-R5, S-R10, S-R15, and S-R20) showed a drop in the uncracked initial stiffness by 4.68%, 5.91%, 8.20%, and 16.06%, whereas a drop in the cracked stiffness by 5.03%, 12.03%, 17.06%, and 25.19%, respectively. While increments of chips rubber to 5%, 10%, 15%, and 20% in specimens (R-R5, R-R10, R-R15, and R-R20) produced a drop in the uncracked stiffness by 2%, 9.46%, 16.33%, and 24.44%, and a drop in the cracked stiffness by 6.96%, 12.25%, 20.36%, and 26.88% respectively**.**

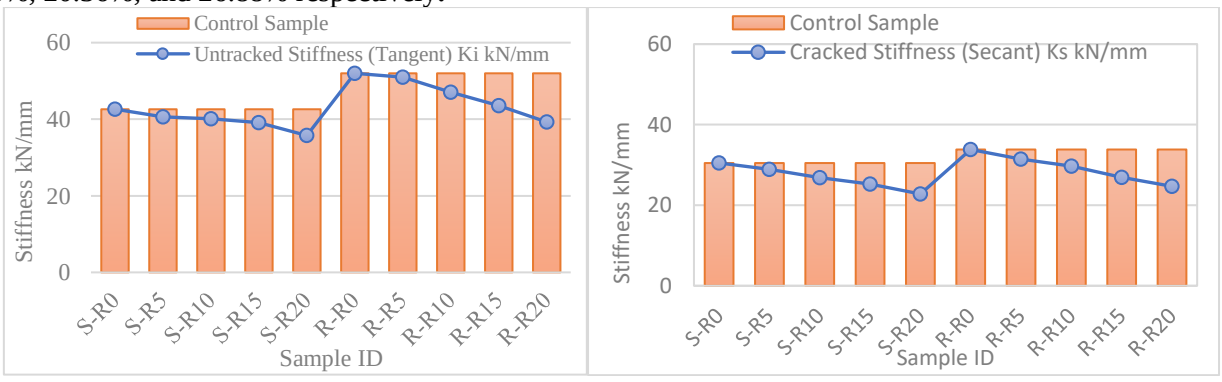

a) Initial stiffness b) Secant stiffness

Figure 10. Effect of rubber chips stiffness of specimens

2.4. Ductility of the tested specimens

Ductility plays a major role in reinforced of structural concrete members designed for seismic zones. These members should have the capacity to sustain load under high deformations allow the evacuation of people while an earthquake occurred. Marzouk and Hussein [26] provided a general description of ductility as the ratio between the displacement was taken at the ultimate load (Δu) and the displacement was taken at the first yielding of the flexure reinforcement (Δy). The definition of yield displacement often time makes it difficult, that is because the load-displacement relationship may not have a well-defined yield point. This may show, e.g., because of the non-linear conduct of the material or because the yield path in a different part of the structure starts at a different loading level [27]. Thus, the process, which given in the previous paragraph, was followed here to estimate of the yielding displacement. The ductility's of all specimens as tabulated in Table 9. Figure 11 explains the considered approach in these determinations. It was observed that adding chips rubber with 5%, 10%, 15%, and 20% increasing the ductility of the specimens S-R5, S-R10, S-R15, and S-R20 by 5.53%, 13.76%, 17.83%, and 20.38%, respectively as shown in Figures 12. while the results proved that the chips rubber with 5%, 10%, 15%, and 20% increases the ductility of the specimens R-R5, R-R10, R-R15, and R-R20 by 4.89%, 6.08%, 9.30%, and 15.60%, respectively as illustrated in Figures 12.

Table 9. Displacement ductility index of all specimens

Group NO.	Specimen	Ultimate Displacement	Yielding Displacement	Displacement Ductility Index
		Δu	Δy	μ
		mm	*mm*	$\Delta u/\Delta y$
G1	S-R0	6.75	4.66	1.45
G2	S-R5	7.23	4.73	1.53
G3	S-R10	7.58	4.60	1.65
G4	S-R15	7.8	4.57	1.71
G5	S-R20	8.37	4.80	1.74
G1	R-R0	6.02	3.73	1.61
G2	R-R5	6.23	3.68	1.69
G3	R-R10	6.54	3.82	1.71
G4	R-R15	6.88	3.90	1.76
G5	R-R20	7.50	4.02	1.87

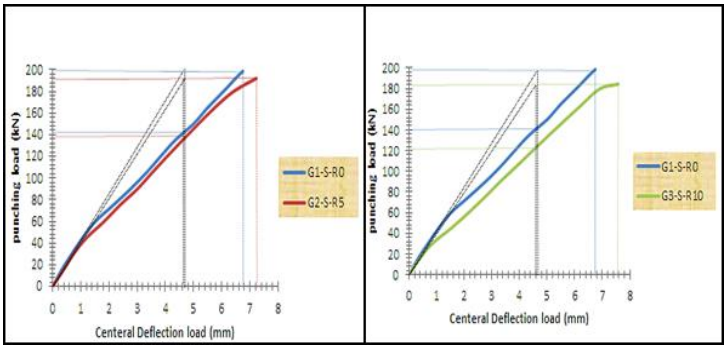

a- Compare S-R5 with S-R0 b- Compare S-R10 with S-R0

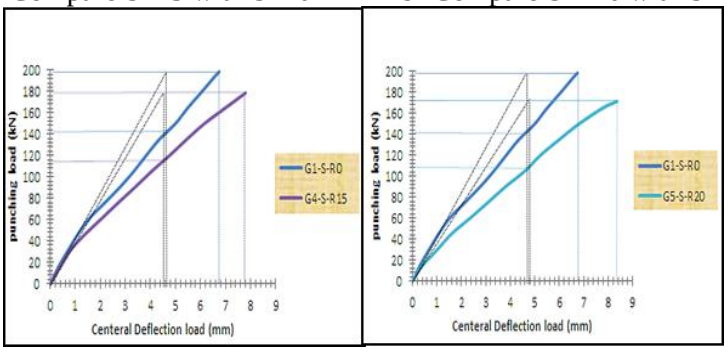

c- Compare S-R15 with S-R0 d- Compare S-R20 with S-R0

Figures 11. Drawing of displacement ductility index of specimens S-R

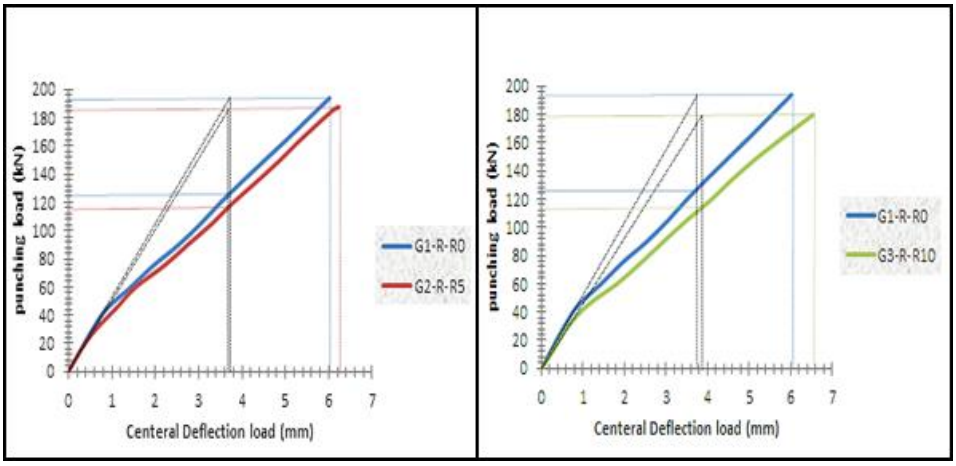

a- Compare R-R5 with R-R0 b- Compare R-R10 with R-R0

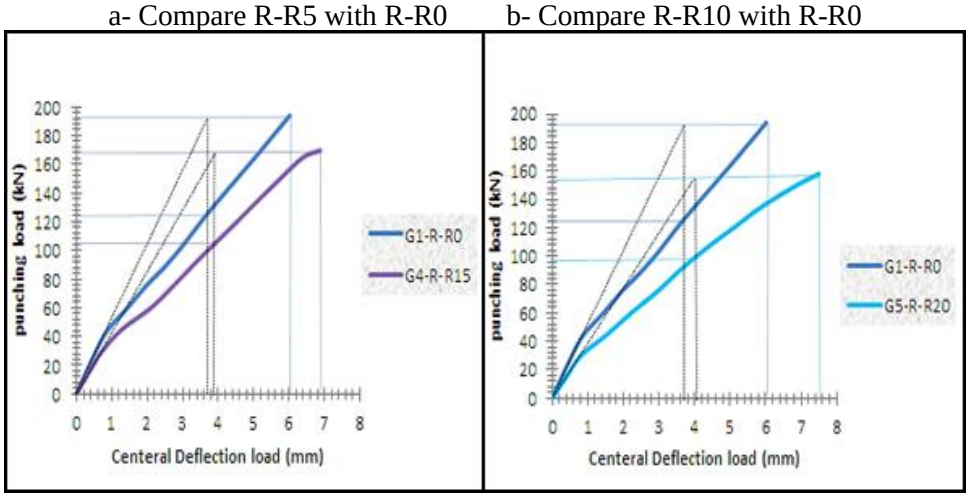

c- Compare R-R15 with R-R0 d- Compare R-R20 with R-R0

Figures 12. Drawing of displacement ductility index of specimens R-R

2.5. Energy absorption of the tested slabs

Husain et al. 2017 [28] defined Energy absorption index (EAI) as the ratio between of the total area under load-displacement diagram to that under the ascending portion only as showed in Figure (13). The limitation of the area under the load-displacement diagram (y= equation of curve) up to the ultimate load for S-R and R-R specimens were characterized in Figure (13a) and Figure (13b) respectively. Results of the energy absorption index of the tested slabs are listed in Table 10.

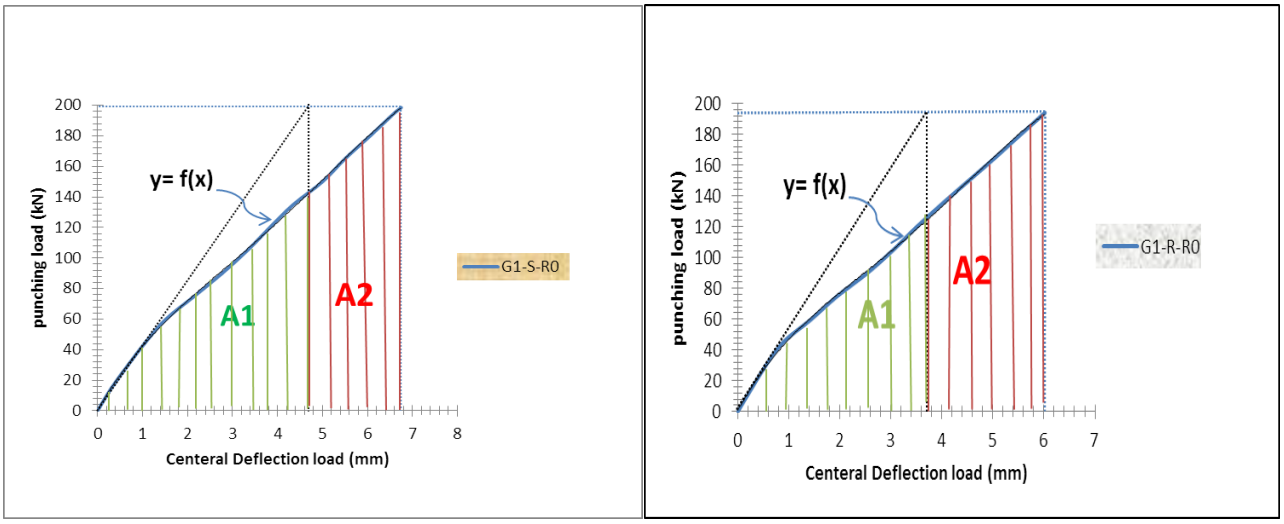

a) S-R0 specimens b) R-R0 specimens

Figure 13. (a) Drawing for computing the EAI

Table 10. Energy absorption-index for all the tested slabs

Group NO.	Specimen	Area under Ascending part	Area under descending part	Total Area	Energy Absorption Index	% Diff. Energy Absorption Index
		A1	*A2*	*A1+ A2*	*EAI*	
		mm^2	*mm^2*	*mm^2*	*(A1+A2)/ A1*	
G1	S-R0	362.52	356.68	719.20	1.98	0.00
G2	S-R5	347.44	422.57	770	2.21	11.61
G3	S-R10	295.20	473.75	768.95	2.60	31.31
G4	S-R15	294.89	482.28	777.17	2.63	32.83
G5	S-R20	286.16	515.58	801.74	2.80	41.41
G1	R-R0	262.31	366.9	629.2	2.40	0.00
G2	R-R5	236.55	389.21	625.75	2.65	10.41
G3	R-R10	237.70	402.78	640.48	2.69	12.08
G4	R-R15	223.49	418.85	642.34	2.87	19.58
G5	R-R20	218.15	455.32	673.47	3.09	28.75

It can be observed that the increment in the ratio of chips rubber from zero to 20% produces increments in EAI are equal to 41.41% and 28.75% for S-R and R-R models respectively.

2.6. Theoretical punching capacity of CRC

ACI 318 limitations will be followed to find the requirement expression for estimating the theoretical punching capacity. For two cases, the results are tabulated in Table 11 and appear carefully the effects of chips rubber ratio on the punching load capacity of specimens, the punching resistance of NSC and CRC specimens without shear reinforcement should be verified by checking the shear stresses in a control perimeter d/2 away from the interior column face. The accuracy and applicability of the suggested punching equations which will be given in this section are to be studied by compares their results with the experimental results.

$\emptyset Vc =$ Minimum value from three equations below:

$$\emptyset Vc = 0.75\,\lambda\frac{\sqrt{f'_c}}{3}\,b_0\,d \qquad \text{.....(1)}$$

$$\emptyset Vc = 0.75\left(1+\frac{2}{\beta}\right)\lambda\frac{\sqrt{f'_c}}{6}\,b_0 d \qquad \text{.....(2)}$$

$$\emptyset Vc = 0.75\left(2+\frac{\alpha\, d}{b_0}\right)\lambda\frac{\sqrt{f'_c}}{12}\,b_0 d \qquad \text{.....(3)}$$

Where:

- f'_c = Compressive strength in MPa.
- b_0 = Control perimeter d/2 away from the interior column faces in mm.
  b_0 = 820mm and 820 mm for specimens of S-R and R-R respectively.
- d = 55 mm for all specimens.
- $\beta = \frac{C1}{C2} = \frac{long\ side\ of\ column}{short\ side\ of\ column}$, β = 1, 2 for specimens of S-R and R-R respectively.
- α = 40 for interior column and λ = 1 for normal concrete.

Table 11. Effect of using chips rubber on punching load capacity of specimens

Group NO.	Specimen	Compressive strength	Ultimate Load experimental	Experimental deficiency	Ultimate Load from Eq. (4.1)	Theoretical deficiency	Difference theoretical and experimental results
		f'_c	*Pu*	Diff.	ØVc*	Diff.	Diff.
		MPa	*kN*	%	*kN*	%	%
G1	S-R0	35.26	198.5	0.00	66.95	0.00	0.00
G2	S-R5	32.31	192.05	-3.25	64.09	-4.27	1.02
G3	S-R10	28.58	184.37	-7.12	60.28	-9.96	2.84
G4	S-R15	26.95	178.71	-9.97	58.53	-12.58	2.61
G5	S-R20	24.74	171.62	-13.54	56.08	-16.24	2.70
G1	R-R0	35.26	193.84	0.00	66.95	0.00	0.00
G2	R-R5	32.31	187.52	-3.26	64.09	-4.27	1.01
G3	R-R10	28.58	179.84	-7.22	60.28	-9.96	2.74
G4	R-R15	26.95	169.67	-12.47	58.53	-12.58	0.11
G5	R-R20	24.74	157.94	-18.52	56.08	-16.24	-2.28

*The control value of equations (1, 2, and 3), Eq. (1) gives minimum values always.

The accuracy and applicability of the suggested punching equations which will be given in this section are to be studied by compares their results with the experimental results. Table 12 includes the theoretical results of ultimate load for punching shear capacity calculated by ACI 318- code equations. Theoretical deficiency were calculated as mentioned previously, the increments in ratio of chips rubber to 5%, 10%, 15%, and 20% show a drop in punching shear capacity for any shape of column, while the experimentally results appeared a reduction in the punching load capacity of S-R and R-R specimens by (3.25%, 7.12%, 9.97%, and 13.54%) and (3.26%, 7.22%, 12.47%, and 18.52%) for ratios of chips rubber 5%, 10%, 15%, and 20% respectively, as illustrated in Figure (14a) and Figure (14b) respectively.

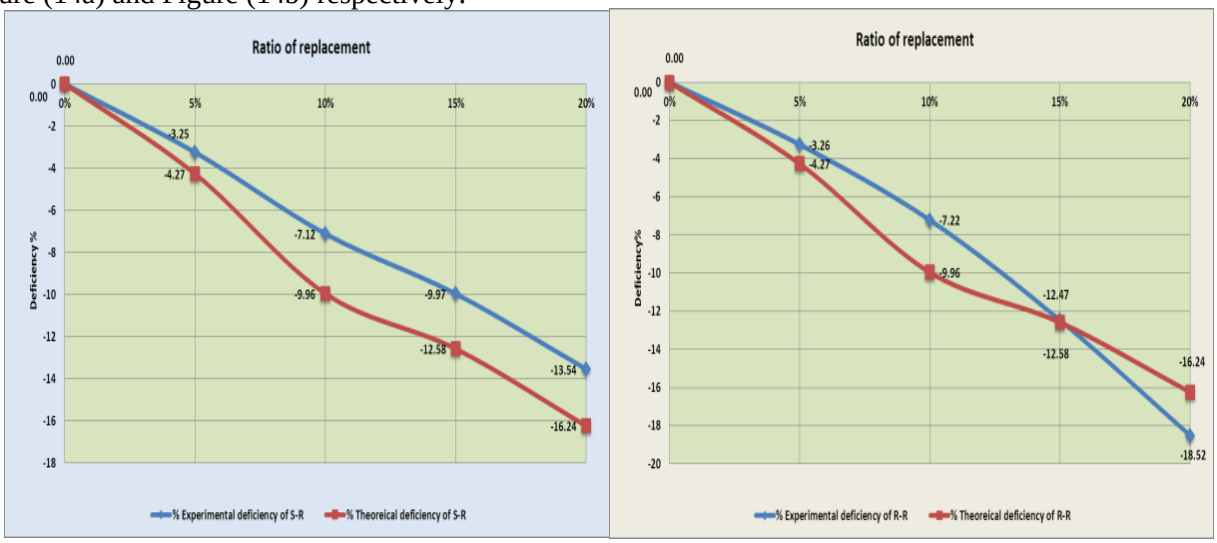

a) S-R specimens b) R-R specimens

Figure 14. Theoretical and experimental deficiency

It can be concluded from comparison of these results the difference between theoretical and experimental results by increasing the ratio of rubber to 5%, 10%, 15%, and 20% in specimens S-R, R-R, are (1.02%, 2.84%, 2.61%, and 2.70%) and (1.01%, 2.74%, 0.11%, and -2.28%) respectively. From the above, evidenced the following:

1. The punching strength of CRC of square shapes is better than the rectangular shapes for replacement 10%, 15%, and 20%, the two cases have the same perimeter.
2. At 20% replacement the maximum decrements in the punching strength were 13.54% and 18.52% for S-R and R-R specimens respectively.

3. Comparison between theoretical and experimental deficiencies reveals that the ultimate failure load calculated according to the ACI-code equation gave diverged results than the experimental results according to the replacement ratio of chips rubber instead of coarse aggregate because the type of this concrete selected for research is CRC. However, for all cases, the equations of ACI-code can be used for replacement equal and less 15% and represented more conservative, but for replacement 20% they are required adjustment, as shown in Figure 14a and 14b.
4. For cases studies shown in Figure 14a and 14b one can find relationship between the percentages of chips rubber ratio represented by x-axis and the deficiency factor % at the punching shear capacity represented by y-axis;

a. Case study NO.1: for flat plate with square column specimens (S-R) model the deficiency equations for experimental and theoretical were as detailed in **Eq. (4a)** and **Eq. (4b)** respectively.

$$y = -22533x^4 + 8946.7x^3 - 1071.7x^2 - 30.967x \quad \ldots\ldots (4a)$$

$$y = -57333x^4 + 23187x^3 - 2758.7x^2 + 1.7333x \quad \ldots\ldots (4b)$$

b. Case study NO.2: for flat plate with square column specimens (R-R) model **Eq. (4.5a)** and **Eq. (4.5b)** represent the experimental and theoretical deficiencies due to rubber replacements.

$$y = 7200x^4 - 2946.7x^3 + 176x^2 - 67.533x \quad \ldots\ldots (5a)$$

$$y = -57333x^4 + 23187x^3 - 2758.7x^2 + 1.7333x \quad \ldots\ldots (5b)$$

From the equations in the previous paragraph, it can be inferred that the experimental results for S-R specimens at all replacement percentages from zero to 20% less constrictive than ACI-code equations, thus ACI- equations can be adopted and represent more conservative, Whereas for R-R specimens the ACI-code equations can be used and also represent more conservative even to replace 15%, after that the correction factor for theoretical equations (ACI-code) must be used; as illustrated in Table 12.

The correction factor can be found by:

$$Correction\ factor = CF = \frac{\text{Theoretical Deficiency}}{\text{Exprimental Deficiency}}$$

CF for S-R model= $\frac{\text{Eq.(4a)}}{\text{Eq.(4b)}}$ **…… (6)** And CF for R-R model= $\frac{\text{Eq.(5a)}}{\text{Eq.(5 b)}}$ **…… (7).**

Finally, the correction factors of less than one for R-R and C-R specimens as illustrated in Table 12, must be used with theoretical ACI-code equations to find punching shear capacity when using rubberized concrete at replacement more than 15%.

Table 12. Correction factor of rubber replacement for three cases.

Chips rubber ratio	Correction factor for S-R Eq.(3)	Correction factor for R-R Eq.(4)
5%	1.314	1.310
6%	1.365	1.404
7%	1.394	1.450
8%	1.408	1.456
9%	1.408	1.430
10%	1.399	1.379
11%	1.381	1.313
12%	1.356	1.237
13%	1.327	1.157
14%	1.294	1.080
15%	1.262	1.009
16%	1.231	0.948
17%	1.207	0.902
18%	1.192	0.872
19%	1.188	0.863
20%	1.199	0.877

4. Conclusions

According to the present experimental data the following conclusions can be outlined:

1. Increasing chip rubber instead of coarse aggregate decreases the punching strength of flat plate, as following: for S-R specimens by 3.25%, 7.12%, 9.97%, and 13.54%, while R-R specimens by 3.31%, 7.27%, 12.51%, and 18.52% when the ratio of replacement is equal to 5%, 10%, 15%, and 20% respectively.

2. Presence of chips rubber increased the ultimate deflection of the specimens. The increments in ultimate central deflection of all slabs were ranged as following: For S-R specimens by 7.11%, 12.30%, 15.56%, and 24%. While for R-R specimens by 3.49%, 8.64%, 14.29%, and 24.58% for replacements 5%, 10%, 15%, and 20% respectively.
3. Generally, increase chip rubber ratio from zero to 5%, 10%, 15% and 20% led to drop the initial and secant stiffness and the reductions ranges in initial and secant stiffness were (16.06% to 28.09%), (25.19% to 30.45%) respectively.
4. Increases the ratio of chips rubber from zero to 20% produces increments in EAI are equal to 41.41% and 28.75% for S-R and R-R models respectively.
5. Using of waste tires chips rubber led to decrease cracks width at failure, and the critical shear crack on the tension side was appeared in a farther location from the column face. Also, the failure mode was changed from a brittle punching to a ductile punching failure. Addition chips rubber at 15% and 20% led a reduction ability to control the spread of the diagonal shear cracks, which caused the whole behavior of the specimen as compared with other specimens.
6. Although NSC specimen's slabs were more effective than CRC in strengthen the punching behavior of slab-column connections, but it has a few disadvantages mainly related with the decreasing in the energy observation index, i.e., poor performance in the little earthquake, may be make CRC one possible solution to improve punching behavior performance.
7. Adding chips rubber instead of coarse aggregate caused increment in the displacement ductility index of specimens reaches to 20.38% and 15.60% for S-R and R-R models respectively.
8. For all cases, the optimum case was at ratio of replacement was between 10% to 15%. For S-R specimens the equations of ACI-code can be used for all percentages of replacements from zero to 20% without correction factor and represent more conservative. While For R-R specimens the equations of ACI-code can be used, but for percentages of replacements more than 15% the correction factor must be used.

References

[1] N. H. FAGHANI and R. EJLALI, "Punching Shear Resistance of High-Strength Concrete Slabs," 2003.
[2] Z. S. Al-Khafaji and M. W. Falah, "Applications of high density concrete in preventing the impact of radiation on human health," *J. Adv. Res. Dyn. Control Syst.*, vol. 12, no. 1 Special Issue, 2020, doi: 10.5373/JARDCS/V12SP1/20201115.
[3] X. Zhang, "Punching Shear Failure Analysis of Reinforced Concrete Flat Plates Using Simplified Ust Failure Criterion," *Sch. Eng. Fac. Eng. Inf. Technol.*, vol. 141, 2002.
[4] H. Sadraie, A. Khaloo, and H. Soltani, "Dynamic performance of concrete slabs reinforced with steel and GFRP bars under impact loading," *Eng. Struct.*, vol. 191, pp. 62–81, 2019.
[5] M. W. Falah, Y. A. Ali, M. Z. Al-Mulali, and Z. S. Al-Khafaji, "Finite Element Analysis Of CFRP Effects On Hollow Reactive Powder Concrete Column Failure Under Different Loading Eccentricity," *Solid State Technol.*, vol. 63, no. 2, 2020.
[6] W. K. Tuama, M. M. Kadhum, N. A. Alwash, Z. S. Al-Khafaji, and M. S. Abdulraheem, "RPC Effect of Crude Oil Products on the Mechanical Characteristics of Reactive-Powder and Normal-Strength Concrete," *Period. Polytech. Civ. Eng.*, 2020, doi: 10.3311/ppci.15580.
[7] P. Mangal, "An Experimental Study On Rubberized Concrete By Using Waste Material With The Addition Of Human Hair As Fiber," *J. Res. Appl. Sci. Eng. Technol.*, vol. 3, no. 9, 2015.
[8] K. Strukar, T. Kalman Šipoš, T. Dokšanović, and H. Rodrigues, "Experimental study of rubberized concrete stress-strain behavior for improving constitutive models," *Materials (Basel).*, vol. 11, no. 11, p. 2245, 2018.
[9] K. Tamanna, M. Tiznobaik, N. Banthia, and M. S. Alam, "Mechanical Properties of Rubberized Concrete Containing Recycled Concrete Aggregate," *ACI Mater. J.*, vol. 117, no. 3, pp. 169–180, 2020.
[10] W. A. Zainab O. Al Masoodi Zainab Al Khafaji, Hassnen M Jafer, Anmar Dulaimi, "The effect of a high alumina silica waste material on the engineering properties of a cement-stabilised soft soil," in *The 3rd BUiD Doctoral Research Conference*, 2017.
[11] Z. S. Al-Khafaji, Z. Al Masoodi, H. Jafer, A. Dulaimi, and W. Atherton, "The Effect Of Using Fluid Catalytic Cracking Catalyst Residue (FC3R)" As A Cement Replacement In Soft Soil Stabilisation," *Int. J. Civ. Eng. Technol. Vol.*, vol. 9, pp. 522–533, 2018.
[12] Z. S. Al-Khafaji, H. K. AL-Naely, and A. E. Al-Najar, "A Review Applying Industrial Waste Materials in Stabilisation of Soft Soil," *Electron. J. Struct. Eng.*, vol. 18, p. 2, 2018.

[13] O. Youssf, M. A. ElGawady, J. E. Mills, and X. Ma, "An experimental investigation of crumb rubber concrete confined by fibre reinforced polymer tubes," *Constr. Build. Mater.*, vol. 53, pp. 522–532, 2014.
[14] M. Küçük and F. Findik, "Selected ecological settlements," *Herit. Sustain. Dev. ISSN 2712-0554*, vol. 2, no. 1, pp. 1–16, Jun. 2020, doi: 10.37868/hsd.v2i1.35.
[15] I. B. Topcu, "The properties of rubberized concretes," *Cem. Concr. Res.*, vol. 25, no. 2, pp. 304–310, 1995.
[16] C. E. Pierce and R. J. Williams, "Scrap Tire Rubber Modified Concrete: Past, Present, and Future," in *Sustainable Waste Management and Recycling: Used/Post-Consumer Tyres: Proceedings of the International Conference organised by the Concrete and Masonry Research Group and held at Kingston University-London on 14-15 September 2004.*, 2004, pp. 1–16.
[17] N. Oikonomou and S. Mavridou, "The use of waste tyre rubber in civil engineering works," in *Sustainability of construction materials*, Elsevier, 2009, pp. 213–238.
[18] N. Segre and I. Joekes, "Use of tire rubber particles as addition to cement paste," *Cem. Concr. Res.*, vol. 30, no. 9, pp. 1421–1425, 2000.
[19] H. Zhong, E. W. Poon, K. Chen, and M. Zhang, "Engineering properties of crumb rubber alkali-activated mortar reinforced with recycled steel fibres," *J. Clean. Prod.*, vol. 238, p. 117950, 2019.
[20] M. Sambucci, D. Marini, A. Sibai, and M. Valente, "Preliminary Mechanical Analysis of Rubber-Cement Composites Suitable for Additive Process Construction," *J. Compos. Sci.*, vol. 4, no. 3, p. 120, 2020.
[21] I. S. IQS, "No. 5, 1984," *Specif. Portl. Cem.*
[22] I. Specification, "No. 45/1984, Aggregates from Natural Sources for Concrete and Construction," *Natl. Cent. Constr. Lab. Res. Baghdad*, 2001.
[23] C. ASTM, "Standard specification for concrete aggregates," *Philadelphia, PA Am. Soc. Test. Mater.*, 2003.
[24] S. Astm, "Standard Specification for Deformed and Plain Carbon-Steel Bars for Concrete Reinforcement ASTM A615/A615M-09b," 2009.
[25] A. C. I. 211 Committee, "Guide for Selecting Proportions for No-Slump Concrete Reported by ACI Committee 211," in *American Concrete Institute*, 2002, vol. 2, pp. 1–26.
[26] H. Marzouk and A. Hussein, "Experimental investigation on the behavior of high-strength concrete slabs," *ACI Struct. J.*, vol. 88, no. 6, pp. 701–713, 1991.
[27] R. Park, "Evaluation of ductility of structures and structural assemblages from laboratory testing," *Bull. new Zeal. Soc. Earthq. Eng.*, vol. 22, no. 3, pp. 155–166, 1989.
[28] M. Husain, A. S. Eisa, and R. Roshdy, "Alternatives to enhance flat slab ductility," *Int. J. Concr. Struct. Mater.*, vol. 11, no. 1, pp. 161–169, 2017.